CLINICS

CLINICAL SCIENCE

Differentiation between tuberculosis and leukemia in abdominal and pelvic lymph nodes: evaluation with contrast-enhanced multidetector computed tomography

Ge Zhang,[I,#] Zhi-gang Yang,[I,II*] Jin Yao,[I,#] Wen Deng,[I] Shuai Zhang,[I] Hua-yan Xu,[I] Qi-hua Long[I]

[I]Sichuan University, West China Hospital, Department of Radiology, Chengdu, Sichuan, China. [II]Sichuan University, West China Hospital, State Key Laboratory of Biotherapy, West China Hospital, Sichuan University, Chengdu, Sichuan, China.

PURPOSE: To compare the characteristics of tubercular vs. leukemic involvement of abdominopelvic lymph nodes using multidetector computed tomography (CT).

MATERIALS AND METHODS: We retrospectively reviewed multidetector computed tomography features including lymph node size, shape, enhancement patterns, and anatomical distribution, in 106 consecutive patients with newly diagnosed, untreated tuberculosis (55 patients; 52%) or leukemia (51 patients; 48%). In patients with leukemia, 32 (62.7%) had chronic lymphocytic leukemia, and 19 (37.3%) had acute leukemias; of these, 10 (19.6%) had acute myeloid leukemia, and 9 (17.6%) had acute lymphocytic leukemia.

RESULTS: The lower para-aortic (30.9% for tuberculosis, 63.2% for acute leukemias and 87.5% for chronic lymphocytic leukemia) and inguinal (9.1% for tuberculosis, 57.9% for acute leukemias and 53.1% for chronic lymphocytic leukemia) lymph nodes were involved more frequently in the three types of leukemia than in tuberculosis (both with $p < 0.017$). Tuberculosis showed peripheral enhancement, frequently with a multilocular appearance, in 43 (78.2%) patients, whereas patients with leukemia (78.9% for acute myeloid leukemia and acute lymphocytic leukemia, 87.5% for chronic lymphocytic leukemia) demonstrated predominantly homogeneous enhancement (both with $p < 0.017$). For the diagnosis of tuberculosis, the analysis showed that a peripheral enhancement pattern had a sensitivity of 78.2%, a specificity of 100%, and an accuracy of 88.7%. For the diagnosis of leukemia, the analysis showed that a homogeneous enhancement pattern was associated with a sensitivity of 84.3%, a specificity of 94.5%, and an accuracy of 89.6%.

CONCLUSION: Our findings indicate that the anatomical distribution and enhancement patterns of lymphadenopathy seen on multidetector computed tomography are useful for differentiating between untreated tuberculosis and leukemia of the abdominopelvic lymph nodes.

KEYWORDS: Tuberculosis; Leukemia; MDCT; Lymph node; Abdomen; Pelvic cavity.

Zhang G, Yang Z, Yao J, Deng W, Zhang S, Xu H, et al. Differentiation between tuberculosis and leukemia in abdominal and pelvic lymph nodes: evaluation with contrast-enhanced multidetector computed tomography. Clinics. 2015;70(3):162-168.

Received for publication on October 10, 2014; **First review completed on** December 3, 2014; **Accepted for publication on** December 28, 2014

E-mail: yangzg666@163.com

*corresponding author

[#]These authors contributed equally to this work and should be considered co-first authors.

INTRODUCTION

According to the World Health Organization, tuberculosis (TB) is the second highest cause of infection-related mortality and was responsible for 1.4 million deaths in 2011 (1). TB remains a major global health challenge due to HIV co-infection, multi-drug resistance, and immigration, especially in many Asian and African countries (2,3). Abdominal TB usually involves the lymph nodes, the genitourinary tract, the peritoneal cavity and the gastrointestinal tract, with lymphadenopathy being its most common manifestation (4,5). Leukemia also infiltrates lymph nodes and may mimic some of the symptoms and clinical signs of TB that involves the abdominopelvic lymph nodes. In some cases, these two diseases present simultaneously or appear successively, which can complicate the diagnosis (6-10). Distinguishing between these two entities is essential for accurate diagnosis and prompt treatment. Multidetector computed tomography (MDCT) has become an ideal diagnostic tool for TB because of its high temporal

No potential conflict of interest was reported.

DOI: 10.6061/clinics/2015(03)02

and spatial resolution and its ability to generate multiplanar reformation (MPR) images. Previously, we found that the distribution and enhancement patterns obtained using MRI or MDCT differed between TB and lymphomas involving the abdominal lymph nodes. These tools were thus helpful for differentiating between the two diseases (11,12). However, there remains doubt as to whether such distribution and enhancement differences also exist between TB and leukemias. To the best of our knowledge, no published studies have compared TB and leukemia of the abdominopelvic lymph nodes using MDCT (13-16). We therefore conducted this study to investigate any potential differences, with the aim being to facilitate more timely and effective treatments.

MATERIALS AND METHODS

Subjects

The Institutional Research Board of our hospital approved the study. Informed consent was obtained from all patients and included information on the possibility of a reaction to the MDCT contrast agent. We retrospectively reviewed 55 consecutive patients who visited our hospital from January 2008 to September 2013 with documented abdominal TB, as well as 51 patients who had untreated leukemia involving the abdominal and pelvic lymph nodes. All enrolled patients underwent abdominal and pelvic contrast-enhanced MDCT scanning. No patients had evidence of other neoplastic diseases, opportunistic infections, liver cirrhosis, or surgical history. Patients with treated leukemia or who did not have a definitive TB diagnosis were excluded.

The cohort of untreated TB patients included 21 women and 34 men, with a mean age of 30.3 years (range, 14 to 77 years). Three patients were diagnosed with HIV co-infection. Constitutional symptoms were as follows: vague abdominal pain (n = 28), abdominal swelling (n = 21), low-grade fever (n = 26), night sweats (n = 28), weight loss (n = 20), diarrhea (n = 6), weakness (n = 17) and abdominal mass (n = 2). Disease duration ranged from 2 weeks to 2 months. The final diagnosis of TB was confirmed by bacteriological (n = 8) or histopathological (n = 28) findings or the presence of proven TB at extra-abdominal and extra-pelvic sites that had improved after drug treatment for TB (n = 19).

The cohort of untreated leukemia patients included 14 women and 37 men, with a mean age of 50.9 years (range, 15 to 82 years). Ten patients were diagnosed with acute myeloid leukemia (AML), 9 with acute lymphocytic leukemia (ALL), and 32 with chronic lymphocytic leukemia (CLL). The most frequent clinical signs and symptoms in these patients were as follows: lymphadenopathy or clinically palpable masses in the neck (n = 8); enlargement of lymph nodes in more than one location (jaw, neck, axilla, or groin) or throughout the body (n = 15); fever (n = 11); vertigo (n = 8); weakness (n = 12); back pain (n = 6); and bleeding tendency (n = 6). The diagnosis of leukemia was made by bone marrow biopsy and flow cytometry (FCM) in 47 patients; in the remaining four patients, the diagnosis of leukemia was made by performing a biopsy of the enlarged lymph nodes and a routine blood test.

Scanning parameters

All included patients completed MDCT scanning within 2-3 days of diagnosis. In 43 patients, scanning was performed with a Somatom Sensation 16 16-section scanner (Siemens Medical Systems, Forchheim, Germany) with the following parameters: 120 kV; 100 mAs; rotation time of 0.5 s; collimation of 16 mm × 0.75 mm; pitch of 0.85; thickness of 5 mm and gap of 2 mm. In 42 patients, scanning was performed with a 64-detector-row CT system (Brilliance 64, Philips Medical Systems, Eindhoven, the Netherlands) with the following parameters: 120 kV; 145 mAs; rotation time of 0.42 s; collimation of 64 mm × 0.625 mm; pitch of 0.891; thickness of 5 mm and gap of 2 mm. The remaining 21 patients were scanned using a dual-source CT system (Somatom Definition; Siemens Healthcare, Forchheim, Germany) in single-tube mode, with the following parameters: 120 kV; 200 mAs; rotation time of 0.33 s; collimation of 24 mm × 1.2 mm; pitch of 0.9; thickness of 5 mm and gap of 2 mm. The patients were asked to empty their bowels and drink 500–750 mL water 30 minutes before the scan. Each patient underwent non-enhanced and enhanced scanning of the entire abdomen, from the top of the diaphragm to the inferior margin of the pubic symphysis. After initial non-enhanced scanning, all patients received 80–85 mL of contrast agent (Iohexol, 300 mg iodine/mL; Beijing Beilu Pharmaceutical, Beijing, China), which was injected using an automatic power injector (Stellant D Dual Syringe, Medrad, Indianola, PA, USA) at a rate of 1.8–2.2 mL/s, via a catheter that had been placed in the antecubital vein. Contrast-enhanced images were obtained after a 60-70 s delay.

Review of MDCT images

Two experienced radiologists (both professors, one with 25 years and the other with 30 years of experience in abdominal imaging) who were blinded to the diagnosis independently interpreted the continuous MDCT images on a dedicated workstation (Syngo; Siemens Medical Systems, Forchheim, Germany). Coronal and sagittal MPR images were also generated using a soft-tissue reconstruction algorithm to aid in the interpretation. The CT features of the affected lymph nodes were recorded, including size, shape, enhancement patterns, and anatomical distribution on MDCT. Any discrepancies between the interpretations were resolved by discussion to obtain a consensus decision.

Lymph nodes were observed in the following anatomic regions: the greater omentum; the lesser omentum (including the hepatogastric ligament, hepatoduodenal ligament, hepatic hilus, and splenic hilus); the mesentery; the anterior pararenal space (including the mesenteric root and the peripancreatic region); the upper and lower para-aortic regions (divided by the upper edge of L3); the internal iliac, external iliac, and common iliac regions; and the inguinal region. The short-axis diameter of each lymph node was measured and compared with that of normal abdominal lymph nodes as proposed by Dorfman et al. (17). Lymph nodes that were larger than the normal size were recorded as enlarged.

The enhancement patterns of the enlarged lymph nodes were classified as homogeneous, peripheral, homogeneous mixed with peripheral, or multilocular. Enhancement was considered peripheral when thick, irregular, or thin enhancement of the rim was seen. A combination of homogeneous and peripheral enhancement was considered when some enlarged lymph nodes showed homogeneous enhancement, but other nodes at the same site showed peripheral enhancement. A multilocular appearance was

confirmed when more than three adjacent conglomerate nodes showed peripheral enhancement and low central attenuation; this was considered a subtype of peripheral enhancement that could sometimes be seen in the two enhancement patterns (12). We also observed extranodal sites, such as the liver, the spleen, the kidney, the adrenal gland and the abdominal wall.

Statistical analysis

All statistical analyses were performed using SPSS software (version 20.0 for Windows, SPSS Inc., Chicago, IL, USA). Categorical variables were expressed as numbers (percentages). Comparisons of anatomical distributions and enhancement patterns between the TB group and the two leukemia groups were performed using the χ^2 test or Fisher's exact test. Bonferroni corrections were performed for multiple pairwise comparisons by adjusting the significance level (α). Continuous variables were presented as the mean $\pm$ SD. The comparison of lymph node size between the TB group and the leukemia group was performed using Student's *t*-test. A two-tailed *P-value* <0.05 was considered to be statistically significant.

RESULTS

MDCT manifestations of untreated tubercular lymphadenopathy

Enlarged lymph nodes in the TB group were circular, ovoid and irregular. The diameter of the lymph nodes associated with TB was 1.23 ± 0.56 cm. TB mainly affected lymph nodes in the lesser omentum (60.0%), the mesentery (65.5%), the anterior pararenal space (63.6%) and the upper para-aortic regions (60.0%) (Table 1). Calcification within the nodes was observed on unenhanced CT images in three patients.

The TB group demonstrated three enhancement patterns: peripheral (n = 43, 78.2%) (Figure 1), homogeneous (n = 3, 5.5%), and homogeneous mixed with peripheral (n = 9, 16.4%). Of the 52 patients with peripheral enhancement or homogeneous mixed with peripheral enhancement, 23 (41.8%) had a multilocular appearance (Table 2, Figure 1).

One patient (1.8%) had hepatomegaly; two (3.6%) exhibited sporadic, peripherally enhancing lesions. Additionally, five patients (9.1%) had splenomegaly, eight (14.5%) had scattered peripherally enhancing lesions (Figure 1), and five (9.1%) had unilateral renal involvement. Ascites was detected in seven cases (12.7%), and 29 cases (52.7%) presented with thickening of the parietal peritoneum, the mesentery, and the greater and lesser omentum. Fifteen patients (27.3%) showed circumferential wall thickening in the bowel, and one (1.8%) displayed gastric wall thickening in the distal body. In addition, three patients (5.5%) had psoas abscesses.

MDCT manifestations of untreated leukemia

Analysis revealed that the enlarged lymph nodes were round or ovoid and that some were fused into irregular masses. Their mean diameter was 1.45 ± 0.67 cm. AML and ALL mainly affected lymph nodes in the upper para-aortic region (73.7%), the lower para-aortic region (63.2%), and the groin (57.9%). CLL mainly affected the lymph nodes in the lesser omentum (87.5%), the mesentery (59.4%), the anterior pararenal space (81.3%), the upper and lower para-aortic regions (90.6% and 87.5%, respectively), the external iliac region (53.1%), and the inguinal region (53.1%) (Table 1). No calcifications were identified in the lymph nodes of this cohort of patients.

In patients with AML and ALL, the enlarged lymph nodes on CT showed two enhancement patterns: 15 patients (78.9%) had homogeneous enhancement, whereas four patients (21.1%) had a combination of homogeneous and peripheral enhancement. In patients with CLL, the enlarged lymph nodes on CT also showed two enhancement patterns. In this case, 28 patients (87.5%) had homogeneous enhancement (Figure 2), and four patients (12.5%) had a combination of homogeneous and peripheral enhancement (Table 2).

In the acute leukemia groups (AML and ALL), nine patients (47.4%) had homogeneous hepatomegaly, one (5.3%) had multiple low-density lesions, and nine (47.4%) had splenomegaly; of these, three (15.8%) had low-density lesions. In addition, six patients (31.6%) had simultaneous hepatomegaly and splenomegaly. Mesenteric thickening was observed in one patient (5.3%). One patient (5.3%) had bilateral adrenal gland involvement, one (5.3%) had a low-density lesion in the kidney, and two (10.5%) showed peritoneal thickening and mesenteric thickening. In the CLL group, five patients (15.6%) had homogeneous hepatomegaly, and one (3.1%) had multiple low-density lesions. Twenty-four patients (75.0%) had splenomegaly, of whom three (9.4%) had low-density lesions. Five patients (15.6%) with CLL had simultaneous hepatomegaly and splenomegaly, and one (3.1%) showed mesenteric thickening.

Table 1 - Comparison of anatomic distribution between tuberculosis and leukemias.

Site	TB (n = 55)	Leukemias		P value	
		AL (n = 19)	CLL (n = 32)	TB vs AL	TB vs CLL
Greater omentum	5(9.1)	0(0)	4(12.5)	0.319	0.72
Lesser omentum	33(60.0)	8(42.1)	28(87.5)	0.176	0.007
Mesentery	36(65.5)	5(26.3)	19(59.4)	0.003	0.571
Anterior pararenal space	35(63.6)	9(47.4)	26(81.3)	0.213	0.084
Upper paraaortic region	33(60.0)	14(73.7)	29(90.6)	0.285	0.002
Lower paraaortic region	17(30.9)	12(63.2)	28(87.5)	0.013	0
Common iliac	16(29.1)	6(31.6)	15(46.9)	0.838	0.095
External iliac	8(14.5)	5(26.3)	17(53.1)	0.298	0
Internal iliac	3(5.5)	2(10.5)	7(21.9)	0.598	0.034
Groin	5(9.1)	11(57.9)	17(53.1)	0	0

The numbers in parentheses are percentages. AL = acute leukemias including acute myeloid leukemia and acute lymphocytic leukemia, CLL = chronic lymphocytic leukemia, TB = tuberculosis, NS = not significant.

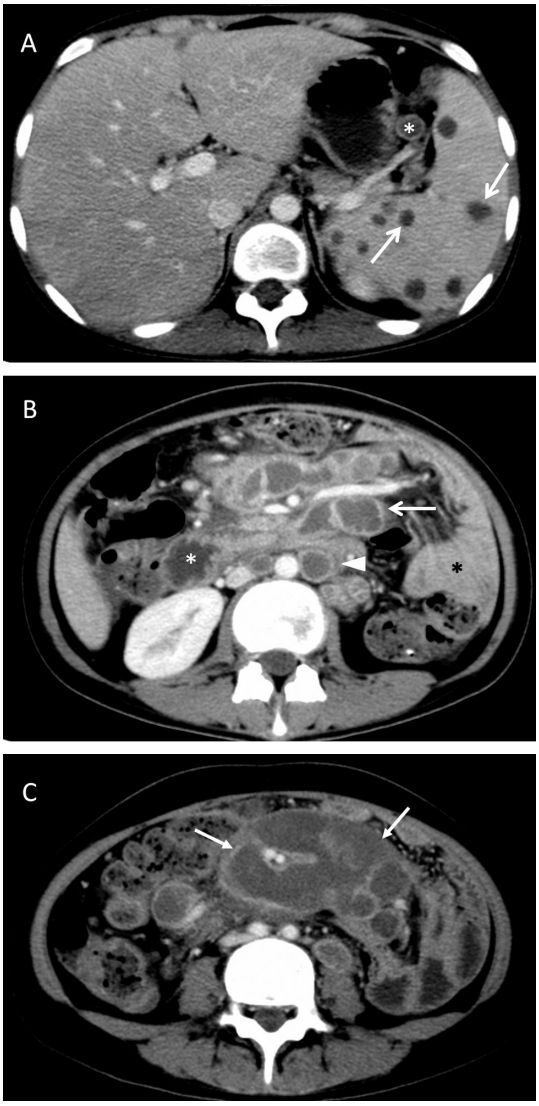

Figure 1 - A 19-year-old female with abdominopelvic and splenic tuberculosis. **A:** A contrast-enhanced image shows peripheral enhancement of enlarged lymph nodes in the splenic hilum (the lesser omentum; star) and sporadic peripheral enhancement lesions in the spleen (arrow). **B:** A contrast-enhanced image shows peripheral enhancement of enlarged lymph nodes in the anterior pararenal space (the mesenteric root; arrow) and the upper para-aortic region (arrowhead). The descending duodenum can be recognized by its mucosal folds (white star). The adjacent intestinal tract shows homogeneous density (black star). **C:** The enlarged lymph nodes demonstrate peripheral enhancement with a multilocular appearance in the mesentery (arrow).

Comparison between untreated TB and leukemia

The diameter of leukemia lymph nodes was larger than those involved with abdominal TB ($p < 0.01$). There was also a statistically significant difference in the anatomical distribution of lymph nodes ($p < 0.017$, Table 1), with the three types of leukemia more frequently involving the lower para-aortic region and the groin.

Peripheral and multilocular enhancement were observed more frequently in patients with TB than in patients with leukemia ($p < 0.01$); patients with leukemia were more likely to have homogeneous enhancement ($p < 0.01$, Table 2).

In cases of TB with a peripheral enhancement pattern, the following measurements were observed: sensitivity of 78.2% (43/55), specificity of 100% (51/51), accuracy of 88.7% (94/106), positive predictive value of 100% (43/43), and negative predictive value of 81.0% (51/63). Similarly, in leukemic patients with a homogeneous enhancement pattern, the following measurements were obtained: sensitivity of 84.3% (43/51), specificity of 94.5% (52/55), accuracy of 89.6% (95/106), positive predictive value of 93.5% (43/46), and negative predictive value of 86.7% (52/60).

DISCUSSION

TB, the second most common life-threatening infectious disease, is usually caused by *Mycobacterium tuberculosis*. Although TB usually affects the lungs, it may cause disease in almost every part of the body, with abdominal TB representing the most common extrapulmonary form (5). Abdominal TB may involve a variety of organs and tissues in the abdomen and may thus mimic many different diseases. The early and accurate diagnosis of this form of TB is therefore especially important. Lymphadenopathy is the most common manifestation of abdominal TB, and sometimes it is the only symptom of the disease (4).

Although biopsy is considered the gold standard for the diagnosis of lymphadenopathy, it is invasive and time-consuming. In contrast, MDCT has the advantage of displaying a broad range of information, including details of specific organ and tissue involvement, in a single examination. This may assist in determining the exact location of an enlarged node before its surgical excision and in evaluating the extent of the disease. In addition, the imaging features of extranodal organs may help differentiate TB from other diseases.

Tuberculous abdominal lymphadenopathy can develop via three main routes. The most common route is the ingestion of infected material containing tubercle bacilli, such as sputum or milk. The second route is the hematogenous spread of bacteria from a distant infection, usually the lungs, and the third route is the direct extension from the serosa of adjacent, involved tissues (14). In the first method of transmission, the bacilli in the lymphoid tissue of the intestinal submucosal layer form epithelioid tubercles. These tubercles drain into the lymphatics of the ileocecum, jejunum, ileum, and the right side of the colon and then to the peripancreatic and superior mesenteric lymph nodes (the anterior pararenal space) at the level of L1, then subsequently to the intestinal trunk, and finally to the cisterna chyli (12,18). Gastric and duodenal involvement of TB is not common, and the bacilli are able to drain into the hepatic hilum, the hepatogastric and hepatoduodenal ligaments, and the peripancreatic region. The lymphatics of the left side of the colon drain to the inferior mesenteric lymph nodes at the level of L3. This route is rarely involved in the dissemination of bacilli; therefore, involvement of the lower para-aortic lymph nodes is rare (12). The inguinal lymph nodes collect lymph mainly from the lower limbs, and they are rarely involved in abdominal TB. In our study, the predominant anatomic distribution of TB was in the lesser omentum (60.0%), the mesentery (65.5%), the anterior pararenal space (63.6%) and the upper para-aortic regions (60.0%), with the exception of the lower para-aortic region (30.9%). This finding is consistent with the known lymphatic drainage routes.

Table 2 - Comparison of enhancement patterns between tuberculosis and leukemias.

Enhancement pattern	TB (n = 55)	Leukemias		P	
		AL (n = 19)	CLL (n = 32)	TB vs AL	TB vs CLL
Peripheral	43(78.2)	0(0)	0(0)	0	0
Homogeneous	3(5.5)	15(78.9)	27(84.4)	0	0
Homogeneous mixed with peripheral	9(16.4)	4(21.1)	5(15.6)	0.729	0.928
Multilocular	23(41.8)	0(0)	0(0)	0.001	0

The numbers in parentheses are percentages. AL = acute leukemias including acute myeloid leukemia and acute lymphocytic leukemia, CLL = chronic lymphocytic leukemia, TB = tuberculosis, NS = not significant.

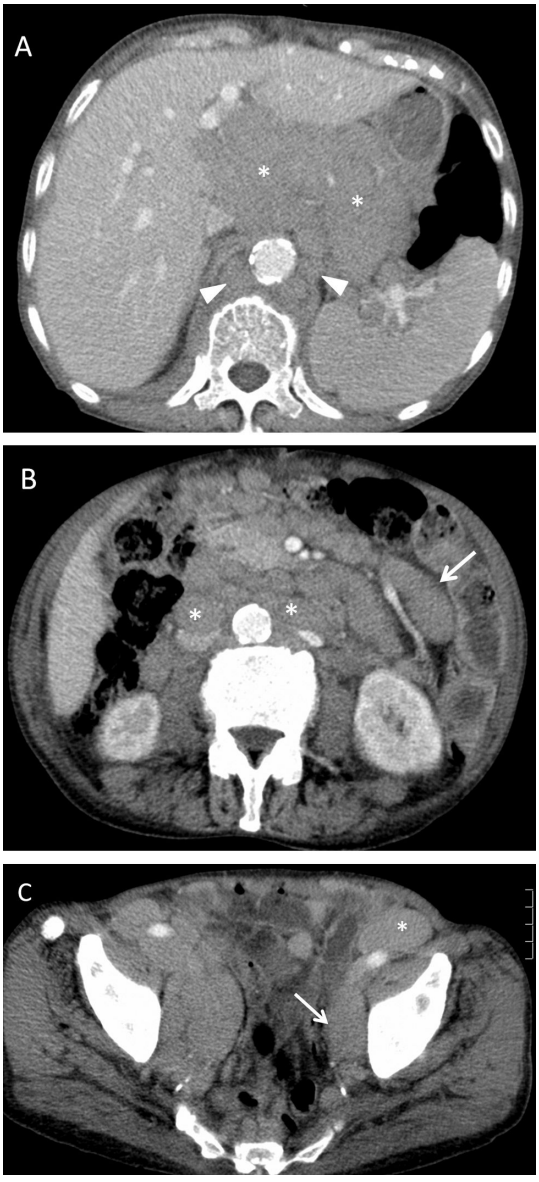

Figure 2 - An 84-year-old man with chronic lymphocytic leukemia. **A:** An enhanced CT image shows homogeneous enhancement of enlarged lymph nodes in the lesser omentum (star) and the upper para-aortic region (arrowhead). **B:** A contrast-enhanced image shows homogeneous enhancement of lymph nodes in the lower para-aortic region (star) and the mesentery (arrow). **C:** The enlarged lymph nodes show homogeneous enhancement in the external iliac (arrow) and inguinal regions (star).

TB-related lymph node enlargement has different stages, which result in different enhancement patterns. In stage one, the lymphoid tissues proliferate and form non-necrotic tubercles and caseating granulomas. In these cases, CT of the lymph nodes shows homogenous enhancement patterns both before and after contrast media injection. In the following stage, the caseating tissues in the center of the lymph nodes display necrosis with intact capsules. Thus, peripheral enhancement can be observed, but the caseating necrosis in the center does not enhance, and the peripheral inflammatory lymphatic tissues show rim enhancement. Once capsular destruction has taken place, periadenitis occurs and adjacent lymph nodes fuse. At this stage, multilocular enhancement is observed. Finally, in the healing stage, lymph node fibrosis and calcification occur. In this stage, calcification of the lymph nodes on plain CT images is sometimes observed (14,18). In our study, 78.2% of cases showed peripheral enhancement, 16.4% showed a combination of homogeneous and peripheral enhancement, 41.8% had a multilocular appearance, and 5.5% showed homogeneous enhancement. Our finding that peripheral enhancement was most frequently observed is consistent with previous studies (13,19,20). In the diagnosis of TB, a peripheral enhancement pattern was associated with a high diagnostic specificity and positive predictive value. All infected nodes measured in our study were less than 4 cm in diameter, consistent with pathologically self-limiting growth.

Leukemia is a group of diseases characterized by the clonal proliferation of abnormal leukocytes presenting in hematopoietic tissues and other organs. Lymphadenopathy is commonly observed in leukemia and is associated with an unfavorable prognosis (21-23). Leukemia is a systemic disease that can cause generalized lymphadenopathy involving more than two noncontiguous regions (23). In our study, the lower para-aortic region and the inguinal lymph nodes were involved more frequently in the three types of leukemias than in TB ($p < 0.017$). The main anatomic sites of involvement in patients with AML and ALL were the upper para-aortic region, the lower para-aortic region, and the groin. In patients with CLL, the lymph nodes in the lesser omentum, the mesentery, the anterior pararenal space, the upper and lower para-aortic regions, the external iliac region, and the inguinal region were more frequently involved. No calcifications were identified in the cohort of leukemia patients. In TB, calcification occurs in the last phase of recovery from inflammation. Leukemic lymphadenopathy is an unlimited clonal proliferation of abnormal leukocytes in lymph nodes with no limitation. These nodes provide an environment that favors the growth and survival of malignant lymphocytes (24), which seems less likely to cause calcification. However, further explanation may be

aided by pathophysiologic investigation of this process. Two enhancement patterns, homogeneous and homogeneous mixed with peripheral, were found in leukemia patients, with the former pattern accounting for the majority (78.9% for acute leukemias and 87.5% for CLL). Intra-nodal necrosis was associated with a heterogeneous enhancement pattern. For the diagnosis of leukemia, a homogenous enhancement pattern provided both high diagnostic specificity and positive predictive values. Lymph node size reflects a balance between cell proliferation and cell death. In leukemia, lymph nodes are generally infiltrated by malignant cells because this location favors their growth and survival and prevents apoptosis (25). In our study, lymph nodes associated with leukemia were larger than those associated with TB ($p < 0.01$).

Enlarged lymph nodes that display a peripheral enhancement pattern also can be observed in other diseases, such as metastatic cancer, Whipple's disease and lymphoma. In metastatic malignancies arising from the testicles, the ovaries or the gastrointestinal tract, a similar pattern is also seen (18). With the primary tumor location and different cell type, a metastatic malignancy can be easily diagnosed. The different treatments adopted for different tumors may also affect their appearance on MDCT. Moreover, the main anatomic distribution of lymph nodes is dependent on lymphatic drainage. Whipple's disease is a systemic infectious disorder that presents with a wide array of symptoms, including migratory arthralgias or arthritis. Symptoms related to nervous system involvement are common, and polymerase chain reaction testing usually is employed to confirm the disease. In some cases, invasive biopsy of the involved tissue (usually a duodenal biopsy) is recommended for a definitive diagnosis (26). A rim-enhancing pattern of lymph nodes in untreated lymphoma also can be observed in MDCT scanning but is rare. After treatment, a rim-enhancing pattern is more commonly observed. According to the study of Shao et al. (11), only 6.9% of lymph nodes show peripheral enhancement in untreated lymphoma. Furthermore, Shao et al. also reported that a homogeneous enhancement pattern can assist in the differential diagnosis of lymphoma and TB, as it has a sensitivity of 69% and a specificity of 96.4%. Further investigations will be required regarding the comparison of CT findings between leukemia and lymphoma of the abdominal and pelvic lymph nodes.

A notable limitation of this study was that in four patients leukemia was not confirmed using bone marrow biopsy and FCM. However, in these patients, the diagnosis was made by lymph node biopsy and blood tests, thereby minimizing this shortcoming. Lymphadenopathy is also observed in chronic myeloid leukemia. However, according to our inclusion criteria that all patients underwent abdominal and pelvic contrast-enhanced MDCT scanning, no such cases were included in this study.

Our study has shown that MDCT can help to differentiate between untreated abdominal TB and leukemia, based on the anatomical distribution and enhancement patterns of lymph nodes. Abdominal TB mainly involved lymph nodes in the mesentery, the anterior pararenal space, the upper para-aortic regions and the lesser omentum. In contrast, the lower para-aortic nodes and the groin lymph nodes were predominantly involved in leukemia. Significant differences in the lymph node enhancement patterns were also observed. In particular, TB lymphadenopathy frequently showed peripheral enhancement with a multilocular appearance, whereas homogeneous enhancement was observed more commonly in leukemia.

ACKNOWLEDGMENTS

The study was supported by the Committee of the National Natural Science Foundation of China (30876088).

AUTHOR CONTRIBUTIONS

Zhang G# is the guarantor of the integrity of the entire study, the literature review, the experimental studies and data analysis, and the preparation and editing of the manuscript. Yang Z contributed to the study concepts and design. Yao J# performed the literature review, the experimental studies and the data analyses. Zhang S performed literature reviews and statistical analyses. Xu H and Long Q performed statistical analyses. Deng W edited the manuscript.

REFERENCES

1. Global tuberculosis control. Geneva: World Health Organization; 2012 (WHO/HTM/TB/2012.6).
2. Valadas E, Antunes F. Tuberculosis, a re-emergent disease. Eur J Radiol. 2005;55(2):154-7.
3. Walls T, Shingadia D. Global epidemiology of paediatric tuberculosis. J Infect. 2004;48(1):13-22.
4. Mathieu D, Ladeb MF, Guigui B, Rousseau M, Vasile N. Periportal tuberculous adenitis: CT features. Radiology. 1986;161(3):713-5, http://dx.doi.org/10.1148/radiology.161.3.3786720.
5. Lee WK, Van Tonder F, Tartaglia CJ, Dagia C, Cazzato RL, Duddalwar VA, et al. CT appearances of abdominal tuberculosis. Clin Radiol. 2012;67(6):596-604, http://dx.doi.org/10.1016/j.crad.2011.11.003.
6. Ker CC, Hung CC, Sheng WH, Chang SC, Luh KT. Fatal mycobacteremia caused by Mycobacterium tuberculosis in a patient with acute leukemia. Leukemia. 1999;13(4):646-7, http://dx.doi.org/10.1038/sj.leu.2401380.
7. Chen CY, Sheng WH, Cheng A, Tsay W, Huang SY, Tang JL, et al. Clinical characteristics and outcomes of Mycobacterium tuberculosis disease in adult patients with hematological malignancies. BMC Infect Dis. 2011;11:324, http://dx.doi.org/10.1186/1471-2334-11-324.
8. Richeldi L, Luppi M, Losi M, Luppi F, Potenza L, Roversi P, et al. Diagnosis of occult tuberculosis in hematological malignancy by enumeration of antigen-specific T cells. Leukemia. 2006;20(2):379-81, http://dx.doi.org/10.1038/sj.leu.2404053.
9. Au WY, Leung AY, Tse EW, Cheung WW, Shek TW, Kwong YL. High incidence of tuberculosis after alemtuzumab treatment in Hong Kong Chinese patients. Leuk Res. 2008;32(4):547-51, http://dx.doi.org/10.1016/j.leukres.2007.06.010.
10. Karanth N, Prabhash KP, Karanth PN, Shet T, Banavali SD, Parikh P. Mediastinal lymphadenopathy in a patient with previously treated T-cell acute lymphoblastic leukaemia. Med J Aust. 2008;188(2):117-8.
11. Shao H, Yang Z-g, Deng W, Chen J, Tang S-s, Wen L-y. Tuberculosis versus lymphoma in the abdominal lymph nodes: A comparative study using contrast-enhanced MRI. Eur J Radiol. 2012;81(10):2513-7.
12. Yang ZG, Min PQ, Sone S, He ZY, Liao ZY, Zhou XP, et al. Tuberculosis versus lymphomas in the abdominal lymph nodes: evaluation with contrast-enhanced CT. AJR. 1999;172(3):619-23, http://dx.doi.org/10.2214/ajr.172.3.10063847.
13. Pombo F, Rodriguez E, Mato J, Pérez-Fontán J, Rivera E, Valvuena L. Patterns of contrast enhancement of tuberculous lymph nodes demonstrated by computed tomography. Clin Radiol. 1992;46(1):13-7, http://dx.doi.org/10.1016/S0009-9260(05)80026-1.
14. Pereira JM, Madureira AJ, Vieira A, Ramos I. Abdominal tuberculosis: Imaging features. Eur J Radiol. 2005;55(2):173-80.
15. Yilmaz T, Sever A, Gür S, Killi RM, Elmas N. CT findings of abdominal tuberculosis in 12 patients. Comput Med Imaging Graph. 2002;26(5):321-5, http://dx.doi.org/10.1016/S0895-6111(02)00029-0.
16. Bankier AA, Fleischmann D, Wiesmayr MN, Putz D, Kontrus M, Hübsch P, et al. Update: Abdominal tuberculosis — Unusual findings on CT. Clin Radiol. 1995;50(4):223-8, http://dx.doi.org/10.1016/S0009-9260(05)83474-9.
17. Dorfman RE, Alpern MB, Gross BH, Sandler MA. Upper abdominal lymph nodes: criteria for normal size determined with CT. Radiology. 1991;180(2):319-22, http://dx.doi.org/10.1148/radiology.180.2.2068292.
18. Vanhoenacker FM, De Backer Al, Op de BB, Maes M, Van Beckevoort D, Kersemans P, et al. Imaging of gastrointestinal and abdominal tuberculosis. Eur Radiol. 2004;14 Suppl 3:E103-15, http://dx.doi.org/10.1007/s00330-003-2047-9.

19. Zhang M, Li M, Xu GP, Liu HJ. Neoplasm-like abdominal nonhematogenous disseminated tuberculous lymphadenopathy: CT evaluation of 12 cases and literature review. World J Gastroenterol. 2011;17(35):4038-43.
20. Kim SY, Kim MJ, Chung JJ, Lee JT, Yoo HS. Abdominal tuberculous lymphadenopathy: MR imaging findings. Abdom Imaging. 2000; 25(6):627-32, http://dx.doi.org/10.1007/s002610000120.
21. Bachh A, Vodarek P, Simkovic M, Motyckova M, Smolej L. 3.6 The role of imaging methods in cll: significant internal lymphadenopathy is frequent and associated with shorter overall survival. Clinical Lymphoma Myeloma and Leukemia. 2011;11, Supplement 2(0):S199-S200, http://dx.doi.org/10.1016/j.clml.2011.09.095.
22. Joshi AD, Dickinson JD, Hegde GV, Sanger WG, Armitage JO, Bierman PJ, et al. Bulky lymphadenopathy with poor clinical outcome is associated with ATM downregulation in B-cell chronic lymphocytic leukemia patients irrespective of 11q23 deletion. Cancer Genet Cytogenet. 2007;172(2):120-6, http://dx.doi.org/10.1016/j.cancergencyto.2006.07.010.
23. Kelly MN, Tuli SS, Usher S, Tuli SY. A 6-Year-Old With Acute-Onset Generalized Lymphadenopathy. J Pediatr Health Care. 2012;26(6):465-70, http://dx.doi.org/10.1016/j.pedhc.2012.07.001.
24. Till KJ, Lin K, Zuzel M, Cawley JC. The chemokine receptor CCR7 and alpha4 integrin are important for migration of chronic lymphocytic leukemia cells into lymph nodes. Blood. 2002;99(8):2977-84, http://dx.doi.org/10.1182/blood.V99.8.2977.
25. Chiorazzi N, Rai KR, Ferrarini M. Chronic lymphocytic leukemia. N Engl J Med. 2005;352(8):804-15.
26. Mohamed W, Neil E, Kupsky WJ, Juhász C, Mittal S, Santhakumar S. Isolated inctracranial Whipple's disease—Report of a rare case and review of the literature. J Neurol Sci. 2011;308(1-2):1-8, http://dx.doi.org/10.1016/j.jns.2011.05.029.